Journal of Marine Science and Technology

Volume 32 | Issue 1 Article 2

Fretting Corrosion Wear of Titanium-Based Alloy (Ti-6Al-4V) in 0.9 wt.% NaCl Solution

Chen-En Lu
Energy College, Quanzhou Vocational and Technical University, China.

Wen-Ken Li
Department of Mechanical Engineering, Chung Yuan University, Taoyuan City 200, Taiwan

Hung-Hua Sheu
Department of Mechanical Engineering, Lunghwa University of Science and Technology, Taoyuan, 333, Taiwan, ROC., hhsheu@mail.lhu.edu.tw

Jeou-long Lee
Department of Semiconductor Engineering, Lunghwa University of Science and Technology, Taoyuan, 333, Taiwan, ROC

Hung-Bin Lee
Department of Optoelectronics and Materials Technology, National Taiwan Ocean University, Keelung 202, Taiwan, ROC, lhb6018@mail.ntou.edu.tw

Recommended Citation

Lu, Chen-En; Li, Wen-Ken; Sheu, Hung-Hua; Lee, Jeou-long; and Lee, Hung-Bin (2024) "Fretting Corrosion Wear of Titanium-Based Alloy (Ti-6Al-4V) in 0.9 wt.% NaCl Solution," *Journal of Marine Science and Technology*: Vol. 32: Iss. 1, Article 2.
DOI: 10.51400/2709-6998.2728
Available at: https://jmstt.ntou.edu.tw/journal/vol32/iss1/2

RESEARCH ARTICLE

Fretting Corrosion Wear of Titanium-Based Alloy (Ti−6Al−4V) in 0.9 wt.% NaCl Solution

Chen-En Lu [a], Wen-Ken Li [b], Hung-Hua Sheu [c,**], Jeou-long Lee [d], Hung-Bin Lee [e,*]

[a] Energy College, Quanzhou Vocational and Technical University, China
[b] Department of Mechanical Engineering, Chung Yuan University, Taoyuan City, 200, Taiwan, ROC
[c] Department of Mechanical Engineering, Lunghwa University of Science and Technology, Taoyuan, 333, Taiwan, ROC
[d] Department of Semiconductor Engineering, Lunghwa University of Science and Technology, Taoyuan, 333, Taiwan, ROC
[e] Department of Optoelectronics and Materials Technology, National Taiwan Ocean University, Keelung, 202, Taiwan, ROC

Abstract

In this study, a high-precision fretting tribo-corrosion tester used to analyze the wear and corrosion behavior of Ti alloys in a fretting motion condition. The tester, operated in a ball-on-plate mode, was employed in the fretting corrosion study of metallic bio-materials (Ti and Ti−6Al−4V) under different loads (0 and 10 N), electrolytes (0.9 wt% NaCl and SBF) and fixed displacement frequency (1 Hz). Using profilometer, optical microscope in the experimental analysis and three-body mechanism in the theoretical analysis, the fretting corrosion performances of these biomedical metals, such as velocity accommodation characteristics, friction, wear, and scratch profile were examined in depth. The dynamic polarization curves indicated that under the same electrolyte and displacement amplitude the mass loss was more severe in fretting corrosion than in simple corrosion. Under different applied potentials −0.5 mV_{SCE}, +0 mV_{SCE} and +1.5 mV_{SCE}, it was found that the friction coefficient and cross-sectional area of worn trace increased with the corrosion potential. Both the mechanisms of adhesive wear and fatigue wear contributed mainly to the wear loss of pure Ti while fatigue wear and abrasive wear were more responsible for the wear loss of Ti−6Al−4V alloy.

Keywords: Titanium, Ti−6Al−4V alloy, Fretting corrosion, Three-body mechanism

1. Introduction

Fretting refers to the extremely small amplitude relative movement of objects in the contact interfaces under interactive loads condition such as mechanical vibration, fatigue load and thermal cycle [1]. Most of the related literatures focus on the research of translational fretting. According to different motion conditions, fretting phenomena can divide into three categories: fretting wear, fretting fatigue, and fretting corrosion [2]. The past literatures focuses on fretting corrosion behavior include calculation and analysis of the stress distribution on the contact surface, fretting corrosion-wear mechanism [3−8]. During fretting -wear process, the metal surface will be harden and the significant plastic flow appear near the surface, the microcracks will form in the subsurface layer where the plastic deformation is constrained and gradually connect with the free surface to form flake metal wear debris, and then gradually split into fine particles. The exposed surface of the metal oxidized, and the extremely fine metal fragments formed during the wear process all oxidized. Therefore, flakes of metal and flocculated oxides are contained in the wear debris formed by fretting wear [9]. Vingsbo et al. [10] proposed the graph concept of fretting process, and considered that the critical point between the adhesion-slip mixed region and the complete slip region is at the lowest point of

Received 2 August 2023; revised 27 November 2023; accepted 29 November 2023.
Available online 11 March 2024

* Corresponding author.
** Corresponding author.
E-mail addresses: hhsheu@mail.lhu.edu.tw (H.-H. Sheu), lhb6018@mail.ntou.edu.tw (H.-B. Lee).

https://doi.org/10.51400/2709-6998.2728

fatigue life. This study did not obtain a mechanism for correct fretting motion response due to experimental space limitations and lack of experimental data validation. In the fretting wear process, two continuous and simultaneous processes can be observed in the form of wear debris formation, i.e. wear debris formation and wear debris evolution. The three-body theory used to explain the change of the friction force-displacement-cycle number (Fr-D-N) curve, and it proposed that the fretting friction coefficient of steel would change with the number of cycles [11,12]. Due to the protective effect of the third body, the adhesion effect suppressed and the friction coefficient is reduced; at this time, the wear debris is continuously formed and removed. When the frequency of the formation and removal of the wear debris reaches an equilibrium stage, the fretting wear enters a stable stage. Zhou et al. [13−16] used different fretting parameters including: load, amplitude, frequency to conduct a basic experiment on Ti−6Al−4V and aluminum alloys, and found that under larger pressure and smaller displacement amplitude, all the friction−displacement curves of metals are closed curves and have a linear relationship. The displacement of the fretting contact surface mainly controlled by the elastic deformation of the metal. Although micro-slip occurs at the contact edge, there is a sticking regime in the contact area, the two contact surfaces do not move relative to each other, and there will be a partial slip zone on the contact surface during the fretting process. On the contrary, when the pressure is small and the displacement amplitude is large, all friction force-displacement curves are open curves, and the curves are in the shape of parallelograms, and the contact surfaces have large relative motion (slip), and the fretting runs in a slip regime. For states between the above test conditions, the obtained friction force-displacement curves vary between linear, elliptical and parallelogram profiles, indicating a change in the fretting state, and this region is called the mixed fretting regime (MFR). In this study, the friction force-displacement plane divided into partial slip area, mixed area and slip area, and two fretting graph theories are established, such as running condition fretting map (RCFM) and material response fretting map (MRFM). It is an important theory used to explain the fretting action and the law of wear. Mischler et al. [17−20] studied the mechanically assisted corrosion behavior (fretting corrosion, tribo-corrosion, etc.) of biomedical metal, focusing on the corrosion behavior of implants of various biomedical metal, especially in high load performance of medical equipment. Through the stiffness of the overall structure and the precision alignment of the parts, a systematic analysis method involving frictional corrosion in metal-to-metal contact was developed. This method provides detailed quantitative information on fretting corrosion wear and explores the effects of surface, alloy, voltage, load, motion, and dissolution conditions on fretting corrosion wear. This fretting corrosion-wear test development system combines the theories from the two fields of mechanics and electrochemistry, and proposes a theoretical model of corrosion-wear. In 0.9 wt% NaCl solution, the friction coefficient and anodic oxidation of the contact metal surface were measured using electrochemical instrument. The results show that Ti−6Al−4V produces corrosion behavior that seriously affects the fretting reaction. The wear behavior of metal surface is analyzed by applying parameters such as different potentials and oscillation frequencies, and the relationship between metal wear and the applied corrosion potential is explained by the fretting three-body theory. Buciumeanu et al. [21] found that the fretting corrosion and wear properties of Ti−6Al−4V alloys with different contents of hydroxyapatite (HA) were better than that of pure titanium. Ti−6Al−4V alloys were tested for friction corrosion using ball-to-plate wear in artificial saliva at 37 °C under open circuit potential (OCP) conditions with a sliding duration of 1800 s, a load of 1 N and a frequency of 1 Hz. The results confirm that the Ti−6Al−4V alloy is suitable as a human implant material.

Zelders et al. [22] found that there is an interaction in the quantitative description of metal corrosion and wear process, that is, corrosion can accelerate wear, and wear can also promote corrosion, which in turn accelerates metal damage. In 1990, the corrosion and wear test method has been used to study the corrosion and wear behavior of various materials under the friction state in the electrolyte. At present, under the corrosion and wear conditions, three important factors of corrosion, wear and corrosion-wear are quantitatively analyzed to determine the main effect factor of the weight loss of metals. Hong and Pyun [23] pointed out that three factors affecting the weight loss of 304L in the state of corrosion and wear are as follows: $W_{cw} = W_{mech} + W_{diss} + W_{acc}$. Zhang and Fang et al. [24,25] described the volume loss equation of 304 SS and 6061 SS under corrosion and wear conditions as follows: $V = V_w + V_c + \triangle V$, $\triangle V = \triangle V_w + \triangle V_c$. Assi and Böhni [26] indicated that the weight loss equation of 304 and 316L under corrosion-wear state is as follows: $W_{cw} = W_{mech} + W_{el.chem} + W_{corr} + \triangle W$, which shows that the increment of corrosion wear is an important factor for the overall corrosion-wear

process. Lee et al. [27,28] pointed out that in nickel-based alloy coatings with different chromium contents, the chromium contents were 7.15 wt% and 16.98 wt% respectively. A block-on-ring corrosion-wear system was used to explore the effects of different chromium contents on the corrosion-wear behavior of nickel-based alloys. The results show that as the polarization potential increases, the total weight loss of corrosion-wear (W_{total}) of the nickel-based alloy increases significantly. Corrosion-wear interactions account for the majority of overall wear losses. Via the quantitative analysis of corrosion and wear, found that the interaction of corrosion and wear is the main factor for the increase in the value of coating weight loss. Muñoz et al. [29] pointed out that the titanium alloy was tested for corrosion and wear, and then current was measured by Faradays law, the volume loss of the metal can calculate ($V_{total} = V_{chemical} + V_{mechanical}$). The results showed that the alloying elements Al and V in the titanium alloy will reduce the activation and passivation dissolution of titanium element, and significantly reduce the wear under tribo-corrosion conditions resulting in accelerated corrosion. Pakhomov [30] studied the influence of coarse and fine grain sizes on the friction and wear characteristics of titanium metal when used in low-frequency reciprocating motion. The results show that there is a significant difference between grain size refinement and displacement amplitude. Lee [31] indicated that the oxide layer formed by the pits on the surface of titanium alloy reduces the occurrence of adhesive wear and inhibits the plastic deformation of the metal at the edge of the pits. Hard oxide particles accumulate inside the pits that are not oxidized and deformed, thereby reducing abrasive wear.

In recently, there have been major breakthroughs in the research results of fretting corrosion and wear. From the three-body theory to the two fretting graph theories, they can reveal the operating law between the fretting operation mechanism and the material damage mechanism and provide an effective judgment on the wear behavior. At the same time, the interaction between corrosion and wear is the focus of research on corrosion and wear of metal materials, and is the main factor to accelerate the destruction of materials. In this study, based on the theory of three-body theory, fretting diagram theory and interaction, the fretting corrosion and wear mechanism of biomedical metal materials (pure titanium, Ti−6Al−4V) was studied to clarify the relevant mechanism and their influence.

2. Experimental

The wear and corrosion test of Ti alloys of fretting motion were carried out with a high-precision fretting corrosion and wear testing machine (Fig. 1) under a ball on plane contact mode. The operated parameters of fretting corrosion test applied on Ti metal and Ti−6Al−4V alloy including different load (0, 10 N), corrosion condition at 0.9 wt% NaCl solution (simulated the corrosivity of blood or body fluids in animals) and the displacement frequency is 1Hz, the polarization curve was then obtained by scanning from −1.5 to 1.5 V at a scanning rate of 0.5 mV/s. The effects of liquid medium, displacement frequency, load and other factors on fretting corrosion are studied. Then, the regional characteristics, friction characteristics, fretting wear and interaction of fretting operation are analyzed. The anticorrosion ability of the titanium alloy were evaluated by electrochemical measurement with a potentiostat (Zahner-Elektrik GMBH & Co., Germany) in a three electrode system comprising a platinum plate as counter electrode, a saturated calomel electrode (SCE) as reference electrode. The worn surfaces of samples were observed with an optical microscope (MICROTECH M835-LED, Japan). The surface roughness of specimens were measured by a surface roughness tester (Alpha-Step Profilometer, KOSAKA Surfcorder SEF3500, Japan), scanning length is 3 mm with a scanning rate at 0.1 mm/s. Moreover, three different potentials (−0.5 mV_{SCE}, +0 mV_{SCE} and +1.5 mV_{SCE}) were directly applied on specimens during the analysis of fretting corrosion wear, respectively.

The titanium alloy samples are contacted by wear-resistant silicon nitride ceramic balls (Si_3N_4) with a diameter of 8 mm, a surface roughness of Ra = 0.02 μm, and a hardness of HV1500. The maximum displacement amplitude value (Stroke) D is ±1.0 mm, load (Fn) is 10 N, frequency is at 1Hz, electrolyte medium is 0.9 wt% NaCl solution, cycle times is 38,000 times. The fretting corrosion-wear equipment was designed and assembled by our research team, the values of displacement amplitude value (D) and cycle number (N) were recorded using Sigma Plot 10.0 software. The friction force (F) were measured by a load cells that transmitted from the lever beam, record the friction force through the signal processing module and through the computer data acquisition system, and substitute $\mu = F/N$ to obtain the friction coefficient value. The corrosion and wear resistance properties of pure titanium and Ti−6Al−4V were analyzed by a three-

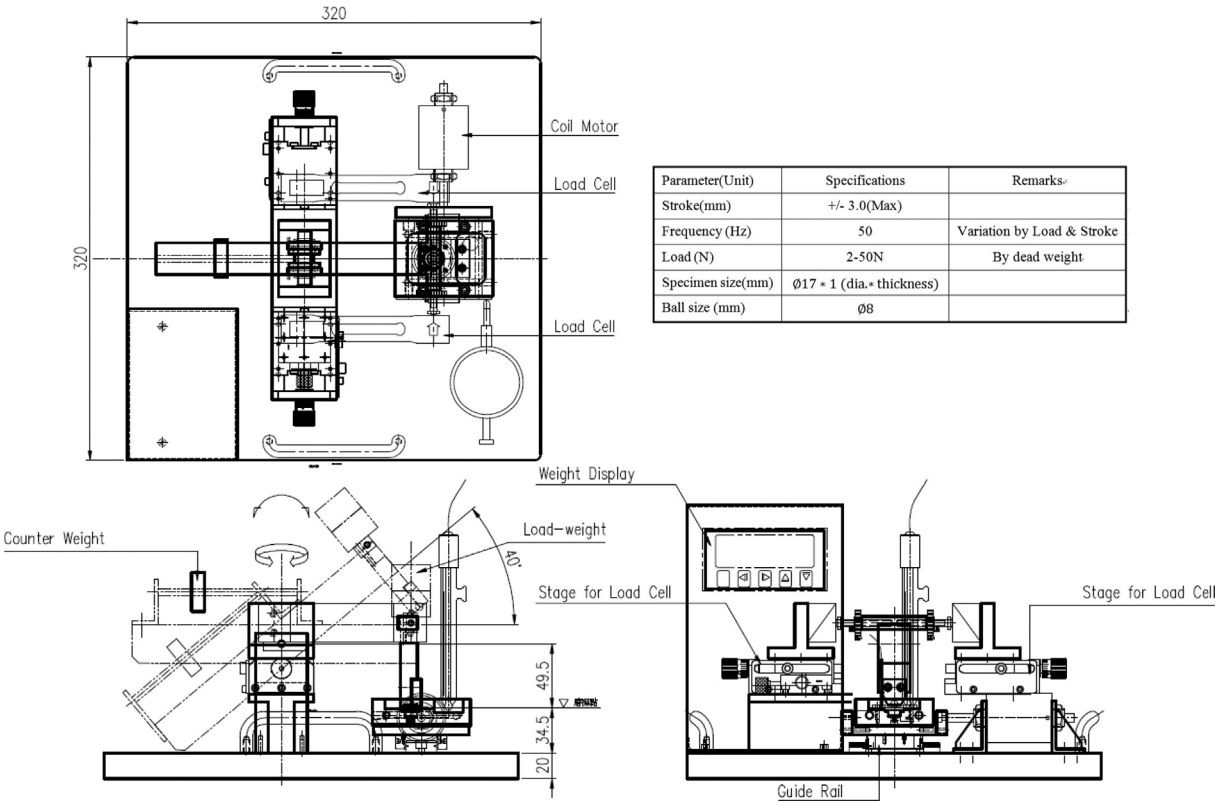

Parameter(Unit)	Specifications	Remarks
Stroke(mm)	+/- 3.0(Max)	
Frequency (Hz)	50	Variation by Load & Stroke
Load (N)	2-50N	By dead weight
Specimen size(mm)	Ø17 * 1 (dia.* thickness)	
Ball size (mm)	Ø8	

Fig. 1. Design drawing of fretting corrosion-wear equipment.

pole system (counter electrode, reference electrode and working electrode) for linear polarization detection. Record and calculate the dynamic friction coefficient (μ) and cycle number (N) curve of the test piece during the experiment, and then complete the three-dimensional relationship curves of Fr-D-N.

3. Results

3.1. Using electrochemistry to investigate corrosion and corrosion-wear reactions

The sample was fixed in the fretting corrosion-wear testing machine, immersed in 0.9 wt% NaCl solution, and the dynamic potential polarization curve was measured. Fig. 2 shows the dynamic polarization curves of pure titanium and Ti−6Al−4V measured under the loading conditions at 0 N and 50 N. From the dynamic corrosion potential polarization curves measured under no-load conditions, it can be observed that both pure titanium and Ti−6Al−4V have the transition behavior of active-→passive→transpassive. The E_{corr} and i_{corr} of pure titanium are −426 mV and 0.56 $x10^{-6}A/cm^2$, respectively. The E_{corr} and i_{corr} of Ti−6Al−4V are −638 mV and 1.22 $x10^{-6}A/cm^2$, respectively. When the dynamic polarization curve of corrosion and wear was measured with a load of 10N, the results showed that the E_{corr} of pure titanium was −473 mV and the i_{corr} was $8.14x10^{-5}A/cm^2$, while the E_{corr} of Ti−6Al−4V was −760 mV and the i_{corr} was $1.56x10^{-5}A/cm^2$. When pure titanium and Ti−6Al−4V are affected by corrosion and wear, the phenomenon that the passivation zone is converted into the overpassivation zone has a shorter corrosion potential range. Conversely, the dynamic polarization curves in the no-wear state show a larger range of passivation potentials for the two metals, which indicates that the growth of the TiO_2 passive film is slower under the no-wear state. From the dynamic potential polarization curve, it can be observed that the corrosion resistance of pure titanium is better than that of Ti−6Al−4V, that is, pure titanium has a relatively low corrosion current density in a corrosive environment. However, compared with pure titanium, Ti−6Al−4V has good mechanical and physical properties, so it is widely used in biomedical applications. However, since Al and V ions will be released in animal's body, it may cause long-term potential health problems, so it is worthwhile to take precautions. When applied a load on the sample, the passivation behavior of the metal surface may be eliminated during friction, leading to the metal continues to expose the fresh surface. This will make the corrosion current value

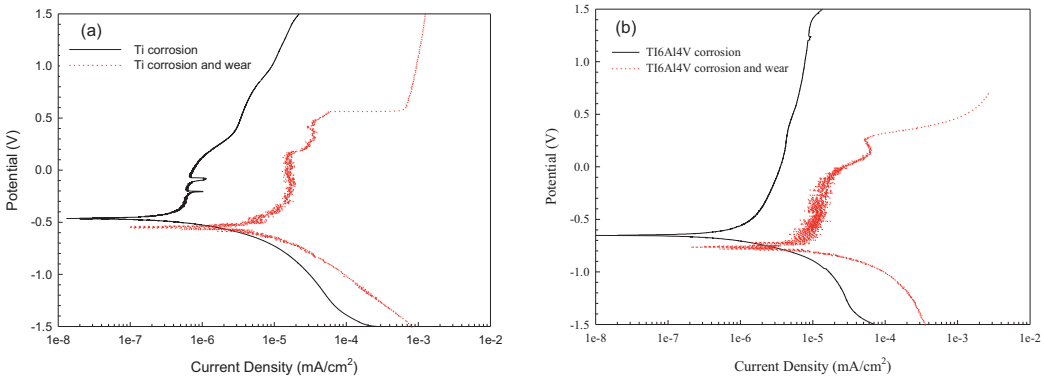

Fig. 2. Polarization curves of pure Ti and Ti−6Al−4V samples measured from 9 wt.% NaCl solution ("corrosion") and 9 wt.% NaCl solution with a friction force 10 N ("corrosion-wear") conditions.

of the metal in the corrosion-wear state slightly higher than that in the pure corrosion state. In this study, three different applied potentials (−0.5 mV_{SCE}, +0 mV_{SCE} and +1.5 mV_{SCE}) were used to analyze the corrosion behavior of pure titanium and Ti−6Al−4V. In general, titanium oxide is a stable substance in neutral solution [32,33]. However, under the different applied potentials, the thickness of the oxide layer formed by pure titanium or titanium alloy may be different [34,35]. Moreover, the composition of the oxide layer formed by pure titanium and Ti−6Al−4V alloy may also change with the action of micro-movement, which is worthy of further investigation.

3.2. Effect of applied potential on fretting corrosion-wear behavior

The three-dimensional graph of friction force (Fr), displacement amplitude value (D) and cycle number (N) is the most important curve showing the characteristics of fretting corrosion wear. According to the curve characteristics and evolution law of friction force and displacement amplitude value, the fretting area of the test piece can be divided into partial slip area, mixed area and slip area. The curve of friction force and displacement amplitude value in the sliding area of the test piece is linear, while the actual wear trajectory of the test piece shows a ring-like feature, but the damage of the test piece is very slight, which usually occurs at the contact edge and is not easy to measure. To obvious surface damage, the mechanics of this wear process conform to Mindlin's theory [8]. In the mixed region, where cracks are rapidly generated in the test piece, cracks exceeding the grain size will be formed, and at the same time, large surface cold work hardening and a small amount of wear debris will be formed. At this time, the curve of friction force and displacement amplitude value is elliptical. In the sliding area, the test piece is worn and a large number of particles are peeled off, so more wear debris accumulation or deep pits can be observed from the cross section of the test piece. At this time, the curve of friction force and displacement amplitude value will present a parallelogram. This area is often characterized by sliding wear along the fretting direction. Fig. 3 shows the Fr-D-N curves of pure titanium immersed in 0.9 wt% NaCl solution under different applied potential conditions (−0.5 mV_{SCE}, +0 mV_{SCE} and +1.5 mV_{SCE}). When the applied voltage at −0.5 mV_{SCE}, as the number of cycles increases, it can be found that the value of friction force and displacement amplitude gradually decreases, and the shape of the curve changes from a quadrangular shape (beginning to wear) to an elliptical shape (6000 cycles), and then to a linear shape (10,000 cycles). This indicates that the deeper the depth of the test piece, the greater the tangential force is, resulting in the smaller displacement amplitude. It can be speculated that the fretting corrosion-wear area is shifted from the slip area to the mixed area and the partial slip area. When the applied voltage is +0 mV_{SCE}, the Fr-D-N curve will change from a quadrangular shape to an elliptical shape (9000 times) and then into a straight shape (13,000 times), which also shows that under the action of this voltage, the deeper the depth of the test piece, the greater the tangential force is, resulting in the smaller displacement amplitude. It also can be speculated that the fretting corrosion-wear area is shifted from the slip area to the mixed area and the partial slip area. When the applied potentials is +1.5 mV_{SCE}, the Fr-D-N curves all show quadrilateral shapes, which indicates that under this voltage, the fretting corrosion-wear area belongs to the slip zone. From the above results, it can be found that when the

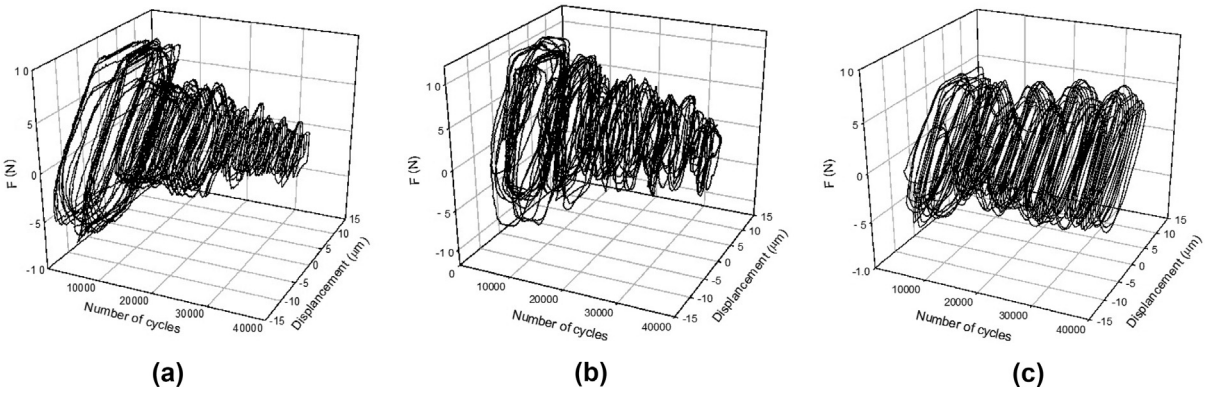

Fig. 3. The Fr-D-N curves of pure Ti samples measured at different corrosion potentials, 0.9 wt% NaCl solution, load 10 N, frequency 1Hz: (a) −0.5mV$_{SCE}$, (b) +0 mV$_{SCE}$, (c) +1.5 mV$_{SCE}$.

applied voltage is larger, the pure titanium specimen will be corroded, the displacement amplitude value range will be larger and the relative friction coefficient will increase with the increase of the displacement amplitude value.

Fig. 4 shows the Fr-D-N curves of Ti−6Al−4V samples immersed in 0.9 wt% NaCl solution under different applied potential conditions (−0.5 mV$_{SCE}$, +0 V$_{SCE}$ and +1.5 mV$_{SCE}$). In the Fr-D-N curve at the applied voltage of −0.5mV$_{SCE}$, it can be observed that with the increase of the number of cycles, the friction force and displacement amplitude value will gradually decrease. The Fr-D-N curve will change from an elliptical shape (beginning to wear) to a linear shape (8000 cycles) indicates that the deeper the depth of the test piece, the greater the tangential force, leading to the smaller the displacement amplitude. At this time, the fretting corrosion-wear operation area turns from the mixed area to the partial slip area.

When the applied potential is +0 mV$_{SCE}$, the Fr-D-N curve will change from a quadrangular shape (beginning to wear) to an elliptical shape (10,000 cycles) and then transform into a straight shape (12,000 cycles). This also shows that under the applied potential of +0 mV$_{SCE}$, the deeper the depth of the test piece, the greater the tangential force is, resulting in the smaller displacement amplitude. It also can be speculated that the fretting corrosion-wear area is shifted from the slip area to the mixed area and the partial slip area. When the applied voltage is +1.5 mV$_{SCE}$, the phenomenon of corrosion-wear behavior of Ti−6Al−4V is as same as the pure Ti. After comparing Figs. 3 and 4, it can be found that the fretting corrosion-wear state will obviously cause wear loss to the material due to electrochemical oxidation reaction. In the slip zone or part of the slip zone, the passivation layer will be removed repeatedly, and then the passivation layer will be formed on the metal surface, resulting in wear loss of the metal.

The anode reacts as follows:

$$Ti + 2H_2O \rightarrow TiO_2 + 4H^+ + 4e^- \quad (1)$$

When the applied voltage is larger, the formation rate of passivation layer of titanium or titanium alloy

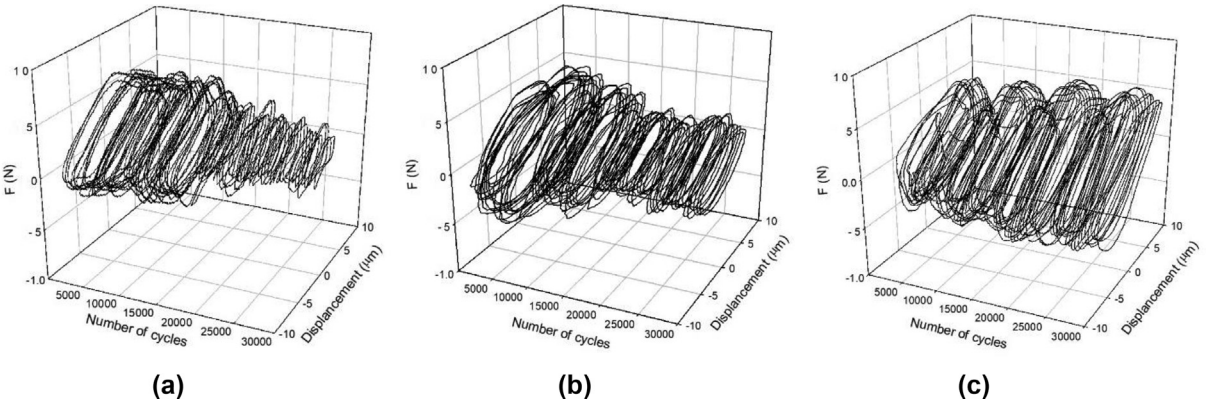

Fig. 4. The Fr-D-N curves of Ti−6Al−4V samples measured at different corrosion potentials, 0.9 wt% NaCl solution, load 10 N, frequency 1Hz: (a) −0.5 mV$_{SCE}$, (b) +0 mV$_{SCE}$, (c) +1.5 mV$_{SCE}$.

is faster. Since the passive layer has the effect of corrosion resistance and lubricity, if the formation rate of passivation film is greater than the wear rate, the friction coefficient of the sample will decrease. The third body theory is used to explain the change of friction force-displacement-cycle number (Fr-D-N) curves obtained from samples corroded with different applied potentials (−0.5 mV_{SCE}, +0 mV_{SCE} and +1.5 mV_{SCE}). The results show that the relationship between the fretting friction coefficient of pure titanium and Ti−6Al−4V and the cycle change is as follows. In the initial stage of fretting, the grinding ball will remove the oxide film on the metal surface, the process time is short and the friction coefficient value of the metal will decrease. When the oxide layer on the metal surface gradually removed, the interaction between the exposed fresh metal surface and the counter-grinding ball increases, and sticking effect occurs in the area of the contact interface, resulting in an increase in the value of the coefficient of friction. Accompanied by work hardening effect, so that the wear debris peels off and forms a third body. When the wear process gradually changes from two-body contact wear to three-body contact wear, the metal surface is protected by the rolling action of the third body, which inhibits the adhesive wear and reduces the friction coefficient of the sample. In the process of continuous formation and removal of wear debris from the contact surface, when the amount of wear debris formed and removed reaches a balance, the fretting wear will enter a stable stage.

It can be observed from the optical microscope metallographic structure photos that the wear pattern and wear rate of the sample will change greatly under the action of different applied potentials. Fig. 3(a) shows that under the applied potential at −0.5 mV_{SCE}, the wear trace on pure titanium is oval with a width of about 4 μm and a length of 8 μm. There are some wear particles accumulated at the end of the wear scar, and the wear scar itself is free of debris from wear, but the roughness of the specimen is reduced. According to the Hertz contact theory [15], it is pointed out that when the contact diameter of the wear track is 148 μm, the maximum pressure that the coating can bear during the wear process is 860 MPa. The wear contact diameter in the Hertz theory is highly correlated with the width of the fretting track. Fig. 5(b) shows that under the condition of applying a potential of +1.5 mV_{SCE}, the fretting scratches left by the sample are larger, and there will be different wear characteristics at the center of the action area and at the edge of the fretting area. The wear scar in the edge of the fretting area will be covered by the passive film, where the measured size of the wear scar is about 10 μm (width) × 8 μm (length). In fact, the observation results by optical microscope show that the wear between the sample and the silicon nitride ceramic ball (Si_3N_4) under the condition of different applied potential and in the fretting contact area will flatten the wear track.

3.3. Influence of fretting time on mechanical and electrochemical properties of samples

The surface roughness of the pure titanium sample under the fretting process at the applied voltage at −0.5 mV_{SCE} was measured, and it was found that there were no obvious dimples formed on the surface of the sample, which indicated that the sample belonged to a partial slip zone during the fretting corrosion process (see Fig. 6(a)). This is consistent with the results of the friction-displacement-cycle number (Fr-D-N) curve explained by the third body theory. The above experimental results are also in line with Mindlin's theory [3], that is, the frictional force (Fr) and the displacement amplitude value (D) in the partial slip zone are linear (Figs. 3(a)−4(a) and 5(a)), and the wear morphology of the sample is

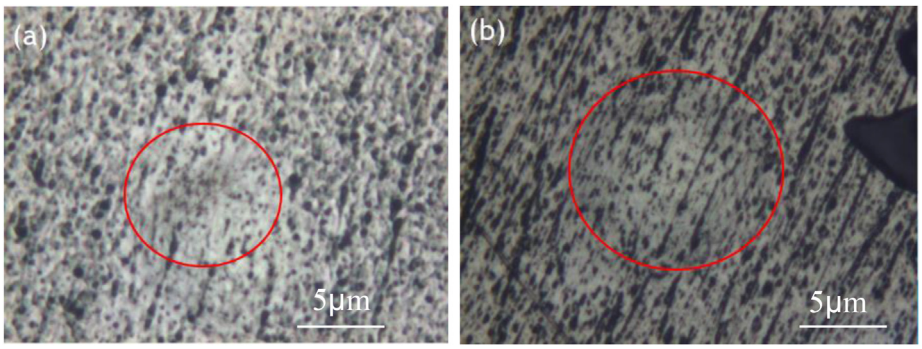

Fig. 5. Morphology of wear scar of pure titanium sample in 0.9 wt% NaCl solution, loaded with 10 N and frequency of 1 Hz (a) −0.5 mV_{SCE}, (b) +1.5 mV_{SCE}.

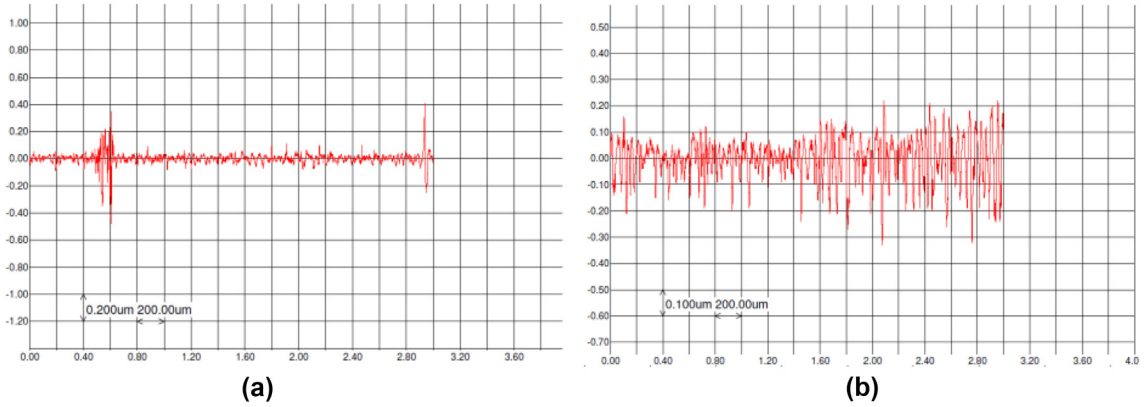

Fig. 6. The surface roughness of samples applied at −0.5 mV_{SCE}, in 0.9 wt% NaCl solution, loaded with 10 N and frequency of 1 Hz: (a) pure Ti, (b) Ti−6Al−4V alloy.

annular. The same result occurred at the Ti−6Al−4V that wear-corrosion at −0.5 mV_{SCE} condition (see Figs. 3(b)−4(b) and 5(b) and Fig. 6(b)). When the applied voltage is +1.5 mV_{SCE}, the friction-displacement-cycle number (Fr-D-N) curve of the sample will show a quadrilateral shape, which means that the fretting corrosion-wear operation area of the sample is all slip zone. Once fretting action start, the current increases significantly, confirming that friction interferes with metal passivation reactions and leads to anodic metal oxidation. At the beginning of friction, the frictional contact area of the sample increases and the metal starts to accumulate and wear. Therefore, the friction-displacement-cycle number (Fr-D-N) curve will present a quadrangular shape and an ellipse in the initial stage, which indicates that the current density will increase significantly in the early stage of corrosion-wear process. In the middle and later stages of corrosion wear, the current density acting on the sample will drop significantly (Fig. 7(a) and (b)).

4. Discussion

The fretting corrosion test device developed in this study is aimed at the study of the fretting corrosion-wear mechanism of biomedical implanted metals (titanium or titanium alloys). The experimental results demonstrate the availability of the device and the detected data for the analysis of fretting corrosion-wear of titanium alloys, and provide theoretical evidence for the complex phenomenon of fretting corrosion [36]. In the electrochemical corrosion environment, fretting corrosion experiments were carried out on pure titanium and Ti−6Al−4V alloys using Si_3N_4 balls. The results show that the interaction between mechanical wear and electrochemical corrosion has obvious correlation. The results in Figs. 3, Figs. 4 and 6 show that there is a correlation between the current change and the linear displacement of wear, which indicates that the electrochemical reaction makes the metal surface prone to third-body wear during the

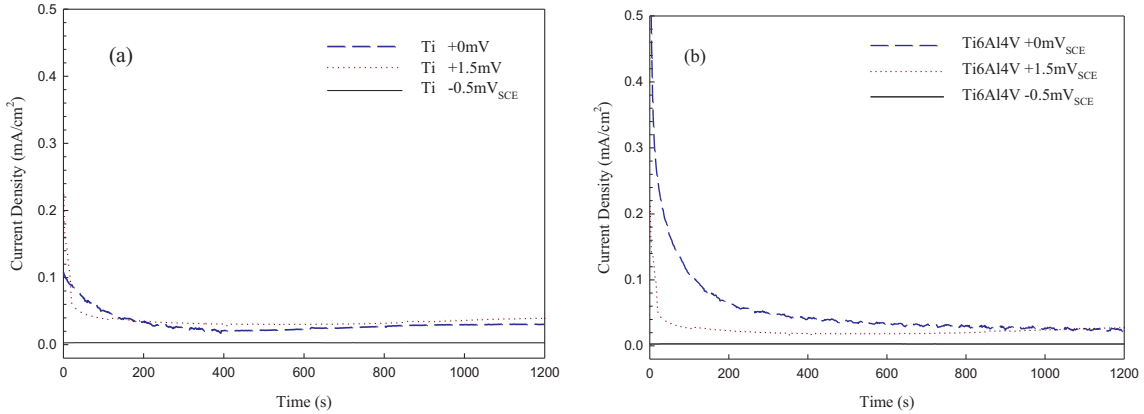

Fig. 7. The relationship between corrosion-wear period and current density curve measured from different applied potentials (−0.5 mV_{SCE}, +0 mV_{SCE} and +1.5 mV_{SCE}), in 0.9 wt% NaCl solution, loaded with 10 N and frequency of 1 Hz: (a) pure Ti, (b) Ti−6Al−4V alloy.

wear process. Moreover, the corrosion current value is related to the cumulative amount of the third body abrasive dander in the process of corrosion-wear, that is, the formation of the third body abrasive particles is related to the process of dissolving and passivating the metal at high current density [17,37]. The third body behavior formed from the oxidation layer wear will be produced periodically from the wear contact surface, leading to a corresponding change in linear wear and friction coefficients. In the process of fretting corrosion, since the passivation layer on the metal surface is constantly worn away and then the new metal surface is constantly forming a passivation layer, the magnitude of the fretting displacement will affect the electrochemical reaction of the metal during fretting corrosion. Therefore, as the displacement amplitude increases, the electrochemical reaction of fretting corrosion is enhanced [38]. In the fretting corrosion-wear experiment, it is known that the chemical corrosion reaction state between metals caused by the friction process will determine the fretting displacement amplitude. This can be attributed to the depassivation rate caused by the oxide film formed during the corrosion process. Therefore, as the displacement amplitude increases, the electrochemical reactivity between the interfaces increases. It can be deduced that the main serious and harmful factors of fretting wear include the following two points: (1) the fretting process will cause the passivation film of the metal to rupture and be difficult to repair. This can be attributed to the small gap between the friction surfaces of metals, resulting in The contact surface is almost at a standstill in motion. In addition, due to the lack of oxygen in the wear area, the metal surface is less likely to undergo a passivation reaction. (2) the fretting process will induce small pits or grooves on the friction surface, causing the corrosive liquid to penetrate and promote pitting and crevice corrosion.

5. Conclusion

In this study, a new experimental device for fretting corrosion-wear mechanism analysis of biomedical metal implants was developed. The experimental results indicate that in the process of fretting corrosion of pure titanium and Ti−6Al−4V samples in corrosive electrolyte, the friction force-displacement-cycle number (Fr-D-N) curve of the samples can be controlled by using different parameters such as applied voltage, load and frequency, and then understand the corrosion mechanism of the sample in the fretting corrosion process. The obtained Fr-D-N curve can illustrate the three-body wear behavior formed during the wear process, and can also predict the correlation between the formation rate and the discharge rate of the three-body wear particles.

Conflict of interest

The authors declare that they have no known competing financial interests or personal relationships that could have appeared to influence the work reported in this paper.

Acknowledgements

The authors thank the Ministry of Science and Technology of the Republic of China, Taiwan, for financially supporting this research under Contract Nos. MOST 110-2221-E-019-027. USTP-NTUT-NTOU-111-03, from National Taipei University of Technology and National Taiwan Ocean University.

References

[1] Waterhouse RB. Pergamon Press Ltd, Oxford 1972;10.
[2] Waterhouse RB. Appl Sci, London 1981.
[3] Mindlin RD. ASME J Appl Mech 1949;16:259.
[4] Uhlig HH. Appl Mech 1954;21:401.
[5] Feng IM, Rightmire BG. Lubr Eng 1954:134.
[6] Hurricks PL. Wear 1970;15:389.
[7] Suh NP. Wear 1973;25:111.
[8] Wharton MH, Waterhouse RB. Wear 1980;62:287.
[9] Gaul DJ, Duquette DJ. Metall Trans A 1980;11:1555.
[10] Vingsbo O, Söderberg S. Wear 1988;126:131.
[11] Godet M. Wear 1984;100:437.
[12] Godet M. Wear 1990;136:29.
[13] Zhou ZR, Fayeulle S, Vincent L. Wear 1992;155:317.
[14] Zhou ZR, Vincent L. Wear 1995;181−183:531.
[15] Zhou ZR, Vincent L. J Tribol 1997;119:36.
[16] Zhou ZR, Nakazawa K, Zhua MH, Maruyama N, Kapsa Ph, Vincent L. Tribol Int 2006;39:1068.
[17] Barril S, Debaud N, Mischler S, Landolt D. Wear 2002;252:744.
[18] Barril S, Mischler S, Landolt D. Wear 2004;256:963.
[19] Barril S, Mischler S, Landolt D. Wear 2005;259:282.
[20] Hiromoto S, Mischler S. Wear 2006;261:1002.
[21] Buciumeanu M, Araujo A, Carvalho O, Miranda G, Souza JCM, Silva FS, Henriques B. Tribol Int 2017;107:77.
[22] Batchelor W, Stachowiak GW. Wear 1988;123:281.
[23] Hong MH, Pyun SI. J Mater Sci Lett 1991;10:716.
[24] Zhang TC, Jiang XX, Li SZ. Wear 1996;199:253.
[25] Fang CK, Huang CC, Chuang TH. Metall Mater Trans A 1999;30:643.
[26] Assi F, Böhni H. Wear 1999;233−235:505.
[27] Lee HB, Hong YH, Sheu HH, Hsiao RC, Li WK, Lin HE. Tribol Int 2023;183:108384.
[28] Lee CY, Lin TJ, Sheu HH, Lee HB. J Mater Res Technol 2021;15:4880.
[29] Dimah MK, Devesa Albeza F, Amigó Borrás V, Igual Muñoz A. Wear 2012;294−295:409.

[30] Pakhomov MA, Gorlov D, Stolyarov V. IOP Conf Ser Mater Sci Eng 2020;996:012017.
[31] Lee HH, Lee S, Park JK, Yang M. Int J Precis Eng Manuf 2018; 19:917.
[32] Kokubo T, Takadama H. Biomaterials 2006;27:2907.
[33] Schmets J, Van Muylder J, Pourbaix M. NACE Cebelcor 1974: 213.
[34] Barril S, Debaud N, Mischler S, Landolt D. Wear 2002;252:744.
[35] Vingsbo O, Söderberg S. Wear 1988;126:131.
[36] Kubacki Bs GW, Sivan S, Gilbert Jeremy L. J Arthroplasty 2017;32:3533.
[37] López-Ortega A, Arana JL, Bayóna R. Wear 2020;456-457: 203388.
[38] Brończyk A, Kowalewski P, Samoraj M. Wear 2020;434−435: 202966.